Journal of Organometallic Chemistry, 478 (1994) 103–110

Geometric features of d^4 metal dicarbonyl monomers with *cis*-π-donor ligands

Joseph L. Templeton, Jennifer L. Caldarelli, Shaoguang Feng, Craig C. Philipp, Michael B. Wells, Brian E. Woodworth and Peter S. White

Department of Chemistry, University of North Carolina, Chapel Hill, NC 27599 (USA)

(Received October 18, 1993)

Abstract

Molecular orbital descriptions for five closely related *cis*-dicarbonyl tungsten(II) d^4 model complexes are presented. The idealized compounds considered are $[H_3W(CO)_2(SH)]^{2-}$, $[H_3W(CO)_2(OH)]^{2-}$, $[H_3W(CO)_2(NH_2)]^{2-}$, $[H_3W(CO)_2(NMe_2)]^{2-}$, and $[H_3W(CO)_2(HC{\equiv}CH)]^-$. These five compounds were chosen to reveal the interplay between the OC–W–CO bond angle and the orientation of a *cis* single-faced π-donor ligand, and the conclusions are based on Extended Hückel calculations. These compounds display similar orientations for the π-donor ligand with respect to the OC–W–CO angle, and each π-donor ligand encounters a barrier to rotation around the tungsten–ligand axis. Coordinates for the computer model $[H_3(CO)_2W(HC{\equiv}CH)]^-$ were based on the results of a single-crystal x-ray diffraction study of $[Tp'W(CO)_2(PhC{\equiv}CMe)][BPh_4]$ (Tp′ = tris (3,5-dimethylpyrazolyl) borate) that is reported here.

Key words: Tungsten; Extended Hückel calculations; Carbonyl; Molecular orbital calculations

1. Introduction

Six coordinate monomers with d^4 configurations present a rich variety of molecular geometries. Angular distortions away from the octahedral paradigm, dominant for d^6 configurations, are the norm for diamagnetic d^4 monomers. A comprehensive theoretical discussion of deformations accessible to d^4 complexes presented by Kubácek and Hoffmann provides an insightful analysis of the roles played by π-effects, σ-effects, and orbital rehybridization in geometrical deformations [1].

Our goal here is more limited in scope, as we restrict our attention to a closely related series of *cis*-dicarbonyl d^4 complexes for which representative examples have only recently become available. The monomers chosen for study here contain the $[W(CO)_2H_3]^-$ fragment, with two *cis*-carbon monoxide ligands, and the sixth coordination site is occupied by a single-faced π-donor ligand. This fragment has been chosen to model the $[Tp'(CO)_2W]^+$ entity (Tp′ = tris(3,5-dimethylpyrazolyl) borate) which is common to the isolated monomers with SR^-, OR^-, NR_2^- and RC≡CR filling the sixth coordination site.

Note that the arguments presented here apply only to the d^4 configuration and are inappropriate for a d^6 complex. Extended Huckel calculations on the $[W(CO)_2H_3]^-$ fragment with the π-base ligands SH^-, OH^-, NH_2^-, NMe_2^-, and HCCH are reported here. The OC–W–CO bond angle and the orientation of the π-donor ligand have been systematically varied to reveal the correlation between these two parameters and to yield rotational barriers. In essence this is a simple application of the general guidelines established by Kubácek and Hoffmann to a specific set of d^4 molecules.

The three facial hydride ligands have been chosen to model Tp′ in this study because of their simplicity. These π-innocent ligands are arranged in a *fac*-geometry around the metal center to approximate the Tp′ ligand which occupies three facial sites in octahedral complexes. Three features of these five complexes are analyzed in this study, and the conclusions are based

Correspondence to: Professor J.L. Templeton.

0022-328X/94/$7.00
SSDI 0022-328X(93)24300-T

on an assessment of electronic features evident in EHMO calculations. These three aspects of the geometries of $[Tp'W(CO)_2]^+$ derivatives which receive attention are (1) the orientation of the single faced π-donor ligand; (2) the angular distortion of the $W(CO)_2$ moiety from 90°; (3) the rotational energy barrier for the π-donor ligand.

2. Experimental details

2.1. Extended Hückel molecular orbital (EHMO) calculations

The calculational method used for this study was the Extended Hückel program on the CAChe (version 3.0) system. Parameters are given in Table 1. All W–C(O) bond distances were set at 1.95, W–H at 1.70 Å and all H–W–H angles were set to 90°. For $[H_3W(CO)_2(OH)]^{2-}$ the W–O bond distance was fixed at 1.95 Å. The W–O–H bond angle was set to 120° with an O–H distance of 0.94 Å. For $[H_3W(CO)_2(SH)]^{2-}$ the W–S–H bond angle was 114.7° with a W–S distance of 2.30 and an S–H distance of 1.35 Å. For $[H_3W(CO)_2(NH_2)]^{2-}$ the WNH_2 fragment is planar with an H–N–H bond angle of 111.0°, a W–N distance of 1.95, and a N–H distance of 1.02 Å. For $[H_3W(CO)_2(NMe_2)]^{2-}$ the C–N–C bond angle was set at 110.1° with a W–N distance of 1.95, a N–C distance of 1.46 and a C–H distance of 1.11 Å. For $[H_3W(CO)_2(HCCH)]^-$ the alkyne C≡C bond distance was set at 1.25 Å, with the center of the alkyne unit 1.95 Å from tungsten. A bent acetylene geometry was idealized with C–C–H angles of 135° and acetylene C–H distances of 1.00 Å.

2.2. Synthesis of $[Tp'W(CO)_2(PhC{\equiv}CMe)][BPh_4]$

$[Tp'W(CO)_2(PhC{\equiv}CMe)][OTf]$ was synthesized using a procedure analogous to that for synthesis of the BF_4^- salt [2] but with $[Ag][O_3SCF_3]$ as the silver cation source rather than $AgBF_4$. Metathesis of the $O_3SCF_3^-$ counterion by BPh_4^- was accomplished by mixing a CH_2Cl_2 solution of $[Tp'W(CO)_2(PhC{\equiv}CMe)][O_3SCF_3]$ with an ethanol solution of $Na[BPh_4]$. Following 1 h of stirring, the solution was filtered and the solvent was evaporated. The residue was washed with ethanol followed by diethylether. Crystals of $[Tp'W(CO)_2(PhC{\equiv}CMe)][BPh_4]$ were grown from CH_2Cl_2/diethylether.

TABLE 1. Parameters used in extended hückel calculations

Atom	Orbital	H_{ii}, eV	ζ_1	ζ_2	C_1	C_2
W	5d	10.37	4.982	2.068	0.6940	0.5631
	6p	5.17	2.309			
	6s	8.26	2.341			
C	2p	11.40	1.625			
	2s	21.40	1.625			
O	2p	14.80	2.275			
	2s	32.30	2.275			
H	1s	13.60	1.300			
S	3d	8.00	1.500			
	3p	11.00	1.827			
	3s	20.00	2.122			
N	2p	13.40	1.950			
	2s	26.00	1.959			

TABLE 2. Crystallographic data collection parameters

	$[Tp'W(CO)_2(PhC{\equiv}CMe)][BPh_4]\cdot 2(CH_2Cl_2)$
Crystal data	
mol formula	$C_{52}H_{54}WB_2O_2N_6Cl_4$
fw	1142.31
cryst dimens, mm	$0.30\times0.30\times0.25$
space group	$P\bar{1}$
cell params	
a, Å	11.401(6)
b, Å	14.301(5)
c, Å	17.252(11)
α, deg	103.78(4)
β, deg	92.85(5)
γ, deg	108.75(4)
V, Å^3	2562.2(24)
Z	2
calcd density, g/cm^3	1.481
Collection and refinement parameters	
radiation (wavelength, Å)	Mo Kα(0.70930)
monochromator	graphite
linear abs coeff, cm^{-1}	25.6
scan type	$\theta/2\theta$
2θ limit, deg	45.0
quadrant collected	$\pm h, +k, \pm l$
total no. of rflns	9505
no. of data with $I \geq 2.5\sigma(I)$	5700
R, %	6.1
R_w, %	7.5
GOF	2.44
no. of params	604
largest param shift/sigma	0.021

2.3. X-ray diffraction data collection for $[Tp'W(CO)_2(PhC{\equiv}CMe)][BPh_4]$

A green block of $[Tp'W(CO)_2(PhC{\equiv}CMe)][BPh_4]$ of dimensions $0.30\times0.30\times0.25$ mm was selected and mounted on a glass wand, and then the crystal was coated with epoxy. Diffraction data were collected on a Rigaku automated diffractometer. Forty six centered reflections found in the region $30.0° < 2\theta < 40.0°$ and refined by least-squares calculations indicated a triclinic cell. The cell parameters are listed in Table 2. Diffraction data were collected in the quadrants $\pm h$, $+k$, $\pm l$ under the conditions specified in Table 2.

TABLE 3. Atomic positional parameters for [Tp'W(CO)$_2$(PhC≡CMe)][BPh$_4$]·2(CH$_2$Cl$_2$)

	x	y	z
W(1)	0.24216(4)	0.09967(3)	0.20330(2)
C(1)	0.3143(10)	0.0362(8)	0.1076(7)
O(1)	0.3634(8)	0.0070(6)	0.0579(5)
C(2)	0.4257(10)	0.1822(8)	0.2453(7)
O(2)	0.5298(7)	0.2195(6)	0.2669(5)
C(3)	0.4045(12)	−0.0537(10)	0.2272(8)
C(4)	0.3054(11)	−0.0090(8)	0.2342(6)
C(5)	0.2043(10)	−0.0077(7)	0.2666(6)
C(11)	0.1253(10)	−0.0572(7)	0.3186(6)
C(12)	0.1592(12)	−0.1249(9)	0.3544(7)
C(13)	0.0884(14)	−0.1640(9)	0.4088(8)
C(14)	−0.0143(13)	−0.1380(10)	0.4288(7)
C(15)	−0.0501(12)	−0.0738(9)	0.3927(7)
C(16)	0.0206(10)	−0.0330(8)	0.3383(6)
B(1)	0.0296(12)	0.2093(10)	0.2023(7)
N(21)	0.0483(8)	0.0372(7)	0.1463(5)
N(22)	−0.0293(8)	0.0966(6)	0.1587(5)
C(23)	−0.1454(10)	0.0393(9)	0.1218(6)
C(24)	−0.1459(10)	−0.0589(8)	0.0843(6)
C(25)	−0.0243(10)	−0.0570(8)	0.1007(6)
C(26)	−0.2501(12)	0.0792(10)	0.1253(7)
C(27)	0.0288(11)	−0.1397(8)	0.0722(7)
N(31)	0.1763(8)	0.1893(6)	0.3032(5)
N(32)	0.0816(8)	0.2231(6)	0.2893(5)
C(33)	0.0568(10)	0.2735(8)	0.3599(6)
C(34)	0.1377(10)	0.2717(7)	0.4204(6)
C(35)	0.2117(10)	0.2195(7)	0.3839(6)
C(36)	−0.0465(12)	0.3177(9)	0.3641(7)
C(37)	0.3104(11)	0.1919(9)	0.4239(6)
N(41)	0.2372(8)	0.2234(7)	0.1505(5)
N(42)	0.1376(8)	0.2568(6)	0.1578(5)
C(43)	0.1505(10)	0.3296(8)	0.1173(6)
C(44)	0.2619(11)	0.3424(8)	0.0846(6)
C(45)	0.3141(10)	0.2776(8)	0.1067(6)
C(46)	0.0595(13)	0.3833(9)	0.1134(7)
C(47)	0.4370(11)	0.2683(10)	0.0871(7)
B(2)	0.5406(11)	0.6957(9)	0.2420(7)
C(51)	0.5981(10)	0.8155(8)	0.2971(6)
C(52)	0.5664(11)	0.8460(8)	0.3736(7)
C(53)	0.6095(12)	0.9480(9)	0.4191(7)
C(54)	0.6851(13)	1.0234(9)	0.3881(8)
C(55)	0.7161(12)	0.9966(9)	0.3120(8)
C(56)	0.6724(11)	0.8932(8)	0.2674(7)
C(61)	0.6400(10)	0.6612(8)	0.1858(6)
C(62)	0.7697(11)	0.7063(8)	0.2066(7)
C(63)	0.8525(11)	0.6680(9)	0.1646(7)
C(64)	0.8103(11)	0.5839(9)	0.1004(7)
C(65)	0.6829(11)	0.5377(8)	0.0770(6)
C(66)	0.6007(10)	0.5764(8)	0.1187(6)
C(71)	0.5129(9)	0.6149(7)	0.2972(6)
C(72)	0.5969(10)	0.6288(8)	0.3658(6)
C(73)	0.5817(10)	0.5558(8)	0.4095(6)
C(74)	0.4827(11)	0.4638(8)	0.3843(6)
C(75)	0.3992(10)	0.4451(8)	0.3177(6)
C(76)	0.4156(10)	0.5192(8)	0.2750(6)
C(81)	0.4123(10)	0.6863(7)	0.1878(6)
C(82)	0.3003(10)	0.6704(8)	0.2193(7)
C(83)	0.1923(11)	0.6686(9)	0.1770(7)
C(84)	0.1925(12)	0.6787(9)	0.1010(8)
C(85)	0.3030(13)	0.6967(10)	0.0670(7)
C(86)	0.4105(11)	0.7001(9)	0.1101(6)
C(91)	0.7367(11)	0.4698(9)	0.2616(7)
Cl(91)	0.7658(3)	0.3679(2)	0.1953(2)
Cl(92)	0.8646(3)	0.5419(3)	0.3372(2)
C(93)	0.3009(13)	0.6083(10)	0.4635(9)
Cl(93)	0.1564(3)	0.5789(3)	0.4085(2)
Cl(94)	0.3452(4)	0.7230(4)	0.5353(3)

Only data with $I > 2.5\sigma(I)$ were used in the structure solution and refinement [3]. The data were corrected for Lorentz-polarization effects during the final stages of data reduction.

2.4. Solution and refinement of the structure

Space group $P\bar{1}$ was confirmed and the position of the tungsten was deduced from the three-dimensional Patterson function. The positions of the remaining non-hydrogen atoms were determined through subsequent Fourier and difference Fourier calculations. Two molecules of methylene chloride were located in the asymmetric unit.

The 67 non-hydrogen atoms were refined anisotropically. The hydrogen atom positions were calculated by using a C–H distance of 0.96 Å and an isotropic thermal parameter calculated from the anisotropic values for the atoms to which they were connected. Final least-squares refinement [4] resulted in the residuals $R = 6.1\%$ and $R_w = 7.5\%$ [5]. The final difference Fourier map had no peak greater than 2.81 e/Å [6].

3. Results and discussion

3.1. X-ray crystal structure of [Tp'W(CO)$_2$(PhC≡CMe)][BPh$_4$]

Atomic positional parameters are listed in Table 3. Selected intramolecular bond distances and angles are listed in Table 4. Molecular drawings of the cation are shown in Figs. 1 and 2 (the BPh_4^- anion has been omitted for clarity). The structure of [Tp'W(CO)$_2$(PhC≡CMe)][BPh$_4$] reveals an acute OC–W–CO angle of 82.9° with the alkyne orientation such that it lies on the molecular mirror plane between the carbonyls. The geometry about the tungsten center approximates an octahedron with the alkyne considered to occupy a single coordination site. The Tp' ligand occupies three facial coordination sites with the two carbonyls and the alkyne occupying the three remaining sites. Although no mirror plane is imposed on the molecular structure by the solid state space group, approximate C_s symmetry is evident by X-ray crystallography, and an effective mirror plane is evident in the ^{1}H NMR spectrum [2].

The alkyne lies between the carbonyls on the symmetry plane of the molecule. The phenyl ring of the

TABLE 4. Selected bond distances (Å) and angles (deg) for $[Tp'W(CO)_2(PhC{\equiv}CMe)][BPh_4]\cdot 2(CH_2Cl_2)$

W-C(1)	2.03(1)	W-N(41)	2.19(1)
W-C(2)	2.04(1)	C(1)-O(1)	1.12(1)
W-C(4)	2.07(1)	C(2)-O(2)	1.14(1)
W-C(5)	2.04(1)	C(3)-C(4)	1.47(2)
W-N(21)	2.18(1)	C(4)-C(5)	1.31(2)
W-N(31)	2.21(1)	C(5)-C(11)	1.45(2)
C(1)-W-C(2)	82.9(4)	C(5)-W-N(21)	89.9(4)
C(1)-W-C(4)	72.2(4)	C(5)-W-N(31)	84.7(3)
C(1)-W-C(5)	103.0(4)	C(5)-W-N(41)	163.6(4)
C(1)-W-N(21)	96.5(4)	N(21)-W-N(31)	86.0(3)
C(1)-W-N(31)	171.9(4)	N(21)-W-N(41)	80.3(3)
C(1)-W-N(41)	91.3(4)	N(31)-W-(41)	81.5(3)
C(2)-W-C(4)	78.1(4)	W-C(1)-O(1)	174.2(9)
C(2)-W-C(5)	102.1(4)	W-C(2)-O(2)	173.4(10)
C(2)-W-N(21)	167.9(4)	W-C(4)-C(3)	144.4(9)
C(2)-W-N(31)	93.1(4)	W-C(4)-C(5)	70.0(7)
C(2)-W-N(41)	87.6(4)	C(3)-C(4)-C(5)	145.5(11)
C(4)-W-C(5)	37.1(4)	W-C(5)-C(4)	72.9(7)
C(4)-W-N(21)	113.3(4)	W-C(5)-C(11)	147.7(8)
C(4)-W-N(31)	113.9(4)	C(4)-C(5)-C(11)	139.4(10)
C(4)-W-N(41)	159.3(4)		

alkyne lies near the two *cis* pyrazole rings of Tp' while the alkyne methyl is near the carbonyls. A weakly attractive π-interaction between the aromatic rings may be present since the alkyne phenyl substituent is proximal to the sterically bulky Tp' ligand. Phenyl substituents seem to favor approach to the Tp' pyrazole rings in a number of molecules [2,7]. The alkyne orientation here maximizes both the alkyne π-donor interaction with the empty d_{yz} orbital of tungsten and the π-acid interaction with the filled d_{xz} orbital of tungsten (*vide infra*). Figure 3 illustrates these interactions. The short W-C(alkyne) distances of 2.07 and 2.04 Å are consistent with a tightly bound four-electron-donor alkyne [8]. The W-C(O) distances are 2.03 and 2.04 Å. The range of W-N distances from 2.18 to 2.21 Å is typical of Tp'W complexes [9].

The acute 82.9° angle formed by the two carbonyls with the tungsten center reflects the energy advantage of increasing overlap of the empty π^* orbitals of the carbonyls with the filled d_{xz} orbital on tungsten. A more detailed bonding description for the metal $d\pi$ interactions in this complex is contained in the molecular orbital discussion which follows.

3.2. Extended Hückel molecular orbital (EHMO) calculations

Extended Hückel Molecular Orbital (EHMO) calculations have been performed on five octahedral tungsten (II) d^4 *cis*-dicarbonyl complexes containing the $[WH_3(CO)_2]^-$ moiety combined with one potential π-base ligand: -SH, -OH, $-NH_2$, $-NMe_2$ or HCCH. Calculations have been performed on this system with the three hydrides in a *fac*-geometry and the carbonyls *cis* to each other with a vacant coordination site *cis* to the carbonyls.

The crucial orbitals in this d^4 system are derived from the octahedral t_{2g} $d\pi$ orbitals. In the coordinate system chosen, rotated 45° in the *xy* plane relative to conventional axes, the $d\pi$ set will consist of d_{xz}, d_{yz} and $d_{x^2-y^2}$. In a low spin d^4 complex, two of these orbitals will be occupied and one will be empty. We

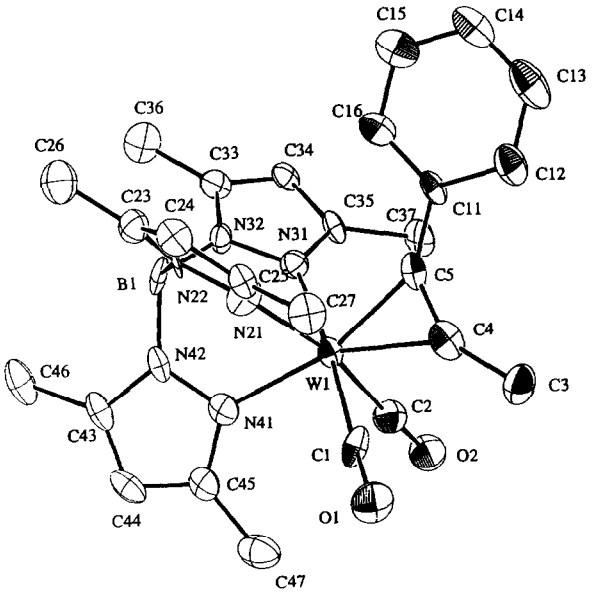

Fig. 1. ORTEP drawing of the $[Tp'W(CO)_2(PhC{\equiv}CMe)][BPh_4]$ complex cation.

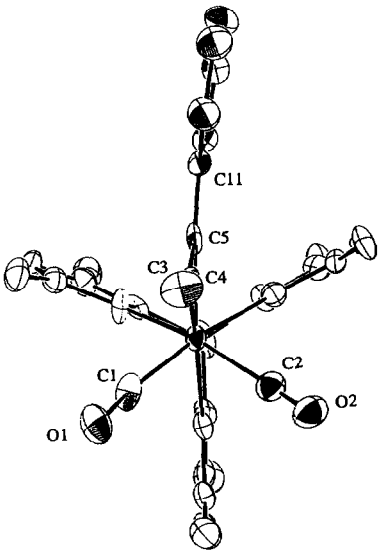

Fig. 2. ORTEP drawing of the $[Tp'W(CO)_2(PhC{\equiv}CMe)][BPh_4]$ complex cation.

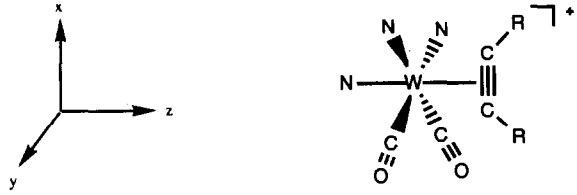

Carbonyl-tungsten interactions:

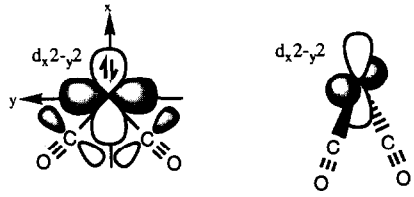

Alkyne-tungsten interactions:

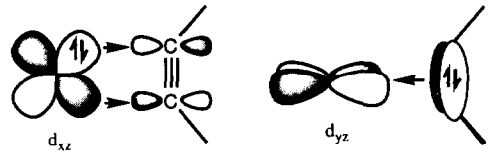

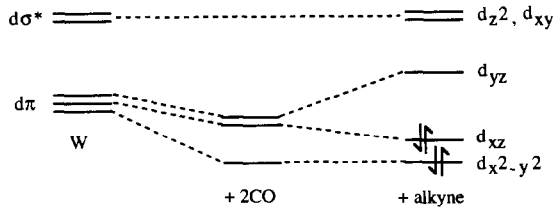

Fig. 3. Qualitative molecular orbital scheme for $[Tp'W(CO)_2(RC{\equiv}CR)]^+$.

will find that the optimal OC–W–CO bond angle hinges on the orientation of the donating electron pair in the p orbital of the unique π-donor ligand which dictates the LUMO and hence defines the occupancy of the $d\pi$ set.

In our system, we have three π-innocent ligands and one π-donor ligand along with the *cis*-dicarbonyl ligands. With a OC–W–CO angle of 90°, the d_{xz} and d_{yz} orbitals are degenerate. As the OC–W–CO bond angle increases or decreases, some net stabilization should be achieved due to increased overlap of the carbonyl π_v^* with the d_{yz} or d_{xz} of tungsten, respectively (Fig. 4). When the orientation of the three hydride ligands was fixed and the OC–W–CO bond angle varied, a double minimum was observed for $H_3W(CO)_2(OH)^{2-}$, $H_3W(CO)_2(NH_2)^{2-}$ and $H_3W(CO)_2(NMe_2)^{2-}$. The orientation of the π-donor ligand can couple with either the acute or obtuse OC–W–CO bond angle to determine the global energy minimum.

The π-base ligands all encounter some barrier to

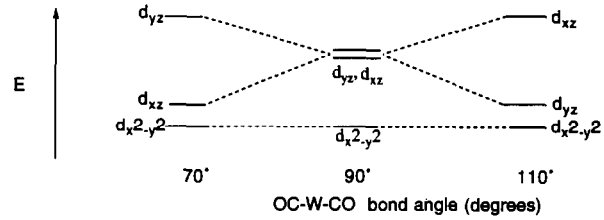

Fig. 4. Qualitative diagram of MO energy dependence on OC–W–CO angle.

rotation according to EHMO results. The main impediment to rotation originates from the filled $p_\perp$ orbital of the π-donor ligand coupling with the vacant LUMO of the tungsten in the ground state. This hinders rotation of the π-base ligand as a redefinition of the LUMO must accompany rotation. The interaction of the $p_\perp$ donor orbital with a $d\pi$ orbital is optimal when the dicarbonyl unit is poised to reinforce the d^4 configuration placement of electrons in the two low lying $d\pi$ orbitals. If the dicarbonyl unit opposes the π-donor ligand by stabilizing the potential $d\pi$ acceptor orbital then this creates an orbital conflict which is reflected in the barrier to rotation as assessed by simple EHMO methods.

3.2.1. $[H_3W(CO)_2(NR_2)]^{2-}$

Consider first the amide complex with an octahedral bonding scheme and a low spin d^4 configuration, such that only two of the three $d\pi$ levels will be occupied. The metal $d_{x^2-y^2}$ orbital overlaps most effectively with both carbonyl π_h^* orbitals, and as a result it is the lowest energy $d\pi$ orbital among the nest of three due to this three-center 2-electron bonding scheme (Fig. 5).

If the two carbonyl ligands were positioned at 90°, a degenerate pair of $d\pi$ orbitals located above $d_{x^2-y^2}$ would result, impacting little on the orientation of the *cis*-π-donor ligand. Reducing this angle from 90° leads to increased π_v^* overlap with d_{xz}, and simultaneously decreases π_v^* overlap with d_{yz} (Fig. 5). Thus for an acute OC–W–CO bond angle the HOMO would presumably be d_{xz}, and d_{yz} would be the LUMO. The vacant d_{yz} orbital is then available to accept electron density and stabilize the filled nitrogen p orbital which is perpendicular to the $W–NR_2$ plane. This stabilization is maximized when the alkyl groups reside in the

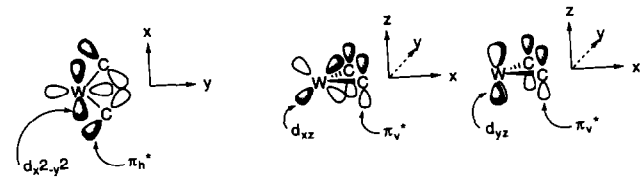

Fig. 5. Metal $d\pi$ interactions with *cis*-di-carbonyl ligands.

xz plane since overlap of p_y with d_{yz} will be optimal at that point.

EHMO calculations were performed to amplify this concept. An octahedral reference point and a planar W–NR_2 group served as the geometric origin for calculations designed to probe the optimal OC–W–CO angle at the four NR_2 orientations resulting from rotations around the W–N bond in 90° increments as shown (Fig. 6).

The results of the EHMO calculations indicated that when W–NR_2 was positioned to give maximum overlap of d_{yz} with the filled $p_\perp$ orbital of nitrogen, at either 0° or 180°, an acute OC–W–CO bond angle is favored. The total energy is indeed minimized by closing the two carbonyl ligands toward d_{yz} with the minimum calculated to be at 81° for the NMe_2 case. Experimentally it has been determined that the Tp'W$(CO)_2$ (NMe_2) complex adopts the anticipated vertical orientation of the dimethylamido ligand between the carbonyl ligands which form an angle of 71.8° at the tungsten center [10].

Conversely, when the NR_2 group is rotated by 90° and the nitrogen $p_\perp$ orbital resides in the xz plane, an obtuse OC–W–CO angle of 99.5° characterizes the global energy minimum for the NMe_2 case. This companion result reflects an increase in the OC–W–CO angle increasing π_v^* overlap with d_{yz} and decreasing overlap with d_{xz}. Clearly this is complimentary to the acute case. Rotational barriers of 14.1 and 11.8 kcal/mol for R = H and R = Me, respectively, were calculated for an OC–W–CO bond angle set at 73°. The change in energy of the HOMO, as the amide ligands were rotated 90°, was greater for the NH_2 case than that for the NMe_2 case. The rotational barrier in each case can be attributed to the $d\pi$ orbital conflict reflected in the HOMO as the NR_2 moiety is rotated around the W–N axis. Since π-bonding from the $p_\perp$ orbital of the π-donor ligand into the vacant $d\pi$ orbital creates a preferred geometry, there is a barrier to rotation. Fixing the OC–W–CO angle and rotating the π-donor ligand and performing EHMO calculations yields a total energy for each geometry, and the difference in total energy between the highest and lowest values may be a reasonable idea of the barrier to rotation. In fact excursions along the energy surface will find the lowest energy pathway through the valleys when the OC–M–CO angle flexes at the same time the π-donor ligand rotates. An experimental rotational barrier of 17 kcal/mol has been reported for the Tp'W$(CO)_2(NH_2)$ complex [11].

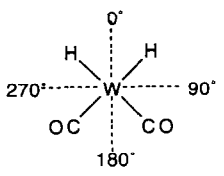

Fig. 6. Coordinate system used (looking down the N–W bond).

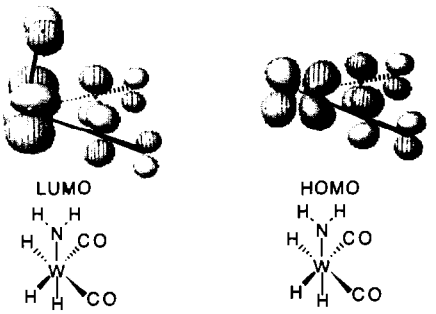

Fig. 7. CACHE representation of HOMO and LUMO of $[H_3W(CO)_2(NH_2)]^{2-}$.

3.2.2. $[H_3W(CO)_2(OH)]^{2-}$

Maximum overlap of d_{yz} with the $p_\perp$ of oxygen yields an acute OC–W–CO bond angle. This occurs with O–H in the xz plane. As the (O)–H unit is rotated towards the yz plane, overlap of $p_\perp$ with d_{yz} decreases and the OC–W–CO bond angle increases. These results are consistent with those observed in the $[H_3W(CO)_2(NR_2)]^{2-}$ complex. When the OH ligand was set at 0° (Fig. 6), an energy minimum resulted at a carbonyl angle of 78°. A surprisingly small rotational barrier of 1.9 kcal/mol was calculated when the OC–W–CO angle was fixed at 73°. This low rotational barrier may reflect the relative reluctance of two-coordinate oxygen to donate an additional lone pair to form a π-bond, or it may be that the W–O multiple bond overrides the OC–W–CO angle influence effectively as it rotates. No experimental data regarding rotation for a hydroxide or alkoxide ligand are available for comparison in this case.

3.2.3 $[H_3W(CO)_2(SH)]^{2-}$

A trend similar to those characteristic of the NR_2^- and OH^- cases is observed here, although the OC–W–CO bond angles minimize at 87.5° when SH is located at 0° (Fig. 6). This is closer to 90° than in the $[H_3W(CO)_2(OH)]^{2-}$ case which is likely due to the sulfur $p_\perp$ orbital being more delocalized and therefore not being stabilized by the vacant $d\pi$ orbital as effectively as with the oxygen $p_\perp$ orbital. Also, the W–S bond distance is 0.35 Å longer than that of W–O, presumably further reducing the impact of π interactions. This decrease in π-interactions is in accord with the general prominence of π-bonds for first row elements with a much smaller role for π-bonding among

the heavier elements. A 6.3 kcal/mole rotational barrier was calculated for the SH ligand. For the related complex $Tp'W(CO)_2(S^iPr)$ an experimental rotational barrier of 16.5 kcal/mol was reported [12]. Note that the structure of $Tp'(CO)_2WSCH_2Ph$ indeed places the thiolate benzyl substituent in the molecular mirror plane between the two carbonyls which subtend an angle of 73.6° [12].

3.2.4. $[H_3W(CO)_2(HCCH)]^-$

With an alkyne as the π-base ligand, binding occurs through σ donation as well as $\pi\|^*$ acceptance and $\pi_\perp$ donation (Fig. 8). It is known that the alkyne will prefer to be *cis* to both carbonyls in order to avoid an orbital conflict between $\pi_\perp$ donation and CO π^* acceptance competing for a shared metal $d\pi$ orbital [8]. As in the previous examples, the orientation of the π-donor ligand hinges on which two $d\pi$ orbitals are filled. Here again an acute OC–W–CO angle will favor placing the π-donor ligand, here the *cis* alkyne, in the plane bisecting the OC–W–CO angle in order for $\pi_\perp$ to encounter the empty d_{yz} orbital and for the $\pi\|^*$ to see the occupied d_{xz} orbital. Alternatively, an obtuse OC–W–CO bond angle reverses the roles of d_{yz} and d_{xz} and leads to an alkyne orientation orthogonal to the OC–W–CO bisector plane in order to minimize the energy. The calculated OC–W–CO angle of 85.5° for the energy minimum for the model alkyne complex $[H_3W(CO)_2(HC{\equiv}CH)]^-$ with the alkyne in the plane bisecting the OC–W–CO angle agrees surprisingly well with the X-ray crystal structure OC–W–CO angle of 82.9° for $[Tp'W(CO)_2(PhC{\equiv}CCH)_3]^+$. Little change in energy is seen in the HOMO and HOMO-1 when the alkyne is rotated by 90°, and a low barrier to rotation of 1.7 kcal/mol was calculated. We believe this small barrier reflects the role of the alkyne $\pi\|^*$ orbital in stabilizing the $d\pi$ orbital it encounters regardless of the OC–M–CO angle. While the variation in energy of the two higher lying $d\pi$ orbitals with the OC–M–CO angle is significant, it is far less dramatic than when $\pi\|^*$ overlaps with a single $d\pi$ orbital, so as the alkyne rotates it simultaneously dictates the HOMO and LUMO to suit its own bonding prescriptions.

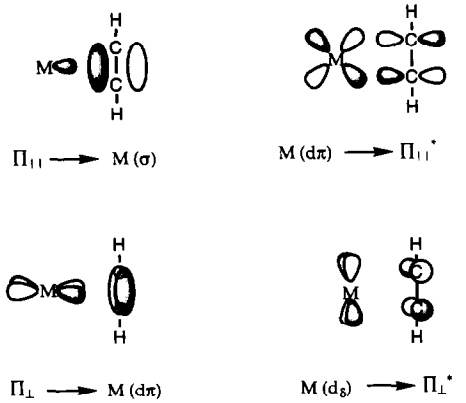

Fig. 8. Metal–alkyne orbital interactions.

4. Summary

Experimental evidence of a correlation between the acute bond angle of a *cis*-dicarbonyl metal moiety and the preferred geometry of a *cis*-π-donor ligand in d^4 metal monomer complexes was the point of departure for this study. Given an OC–W–CO bond angle of 90°, an idealized octahedral geometry, the tungsten d_{xz} and d_{yz} orbitals will be degenerate. As the OC–W–CO angle opens or closes, overlap with one of these two $d\pi$ orbitals increases while overlap with the other orbital decreases, and in a low spin d^4 system, the stabilized $d\pi$ orbital will be filled along with the $d_{x^2-y^2}$ orbital. The destabilized $d\pi$ orbital will be vacant and hence available to accept π-donation. The *cis*-π-donor ligand will be aligned so that the filled $p_\perp$ orbital, the orbital best suited for π-donation, has maximum interaction with the available vacant $d\pi$ orbital. With an acute OC–W–CO angle, the π-donor ligand plane bisects the OC–W–CO angle allowing for $p_\perp$ overlap with the d_{yz} orbital. The experimental results for NR_2^-, SR^-, and RC≡CR conform to this arrangement. Conversely, an obtuse OC–W–CO angle should dictate that the π-donor ligand plane be perpendicular to the OC–W–CO bisector plane allowing for $p_\perp$ overlap with the d_{xz} orbital. By contrast, in a d^6 system, all three $d\pi$ orbitals are filled and there is no orbital available to accept π-donation regardless of ligand orientation factors. Our results, both experimental and theoretical, nicely complement and reinforce the conclusions reported by Kubácek and Hoffmann [1].

Acknowledgments

We thank the Department of Energy, Office of Basic Energy Sciences (85ER13430) for generous support of this research. Tables of complete bond distances and angles, anisotropic temperature factors and observed and calculated structure factors are available upon request from the authors.

References

1 P. Kubácek and R. Hoffmann, *J. Am. Chem. Soc., 103* (1981) 4320.
2 S.G. Feng, A.S. Gamble, C.C. Philipp, P.S. White and J.L. Templeton, *Organometallics, 10* (1991) 3504.
3 Programs used during solution and refinement were from the NCRVAX structure determination package: E.J. Gabe, Y. Le Page,

J.P. Charland, F.L. Lee and P.S. White, *J. Appl. Chem., 22* (1989) 384.

4 The function minimized was $\Sigma w(|F_0| - |F_c|)^2$, where w is based on counter statistics.

5 $R_{\text{unweighted}} = \Sigma(\| F_0 | - | F_c \|)/\Sigma | F_0 |$ and $R_{\text{weighted}} = [\Sigma w(|F_0| - |F_c|)^2/\Sigma w F_0^2]^{1/2}$.

6 Scattering factors were taken from the following: D.T. Cromer, J.T. Waber, in J.A. Ibers and J.C. Hamilton (eds.), *International Tables for X-ray Crystallography: Vol. IV*, Kynoch Press, Birmingham, UK, 1974, Table 2.2.

7 S.G. Feng, P.S. White and J.L. Templeton, *Organometallics, 12* (1993) 2131.

8 J.L. Templeton, *Adv. Organomet. Chem., 29* (1989) 1.

9 S. Trofimenko, *Chem. Rev., 93* (1993) 943.

10 K.R. Powell, P.J. Pérez, L. Luan, S.G. Feng, P.S. White, M. Brookhart and J.L. Templeton, *Organometallics*, in press.

11 P.J. Pérez, L. Luan, P.S. White, M. Brookhart and J.L.Templeton, *J. Am. Chem. Soc., 114* (1992) 7928.

12 C.C. Philipp, C.G. Young, P.S. White and J.L. Templeton. *Inorg. Chem., 32* (1993) 5437.